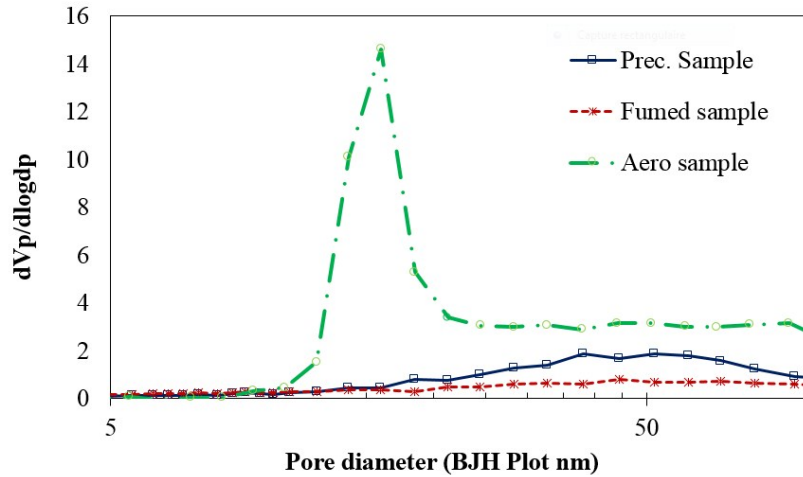


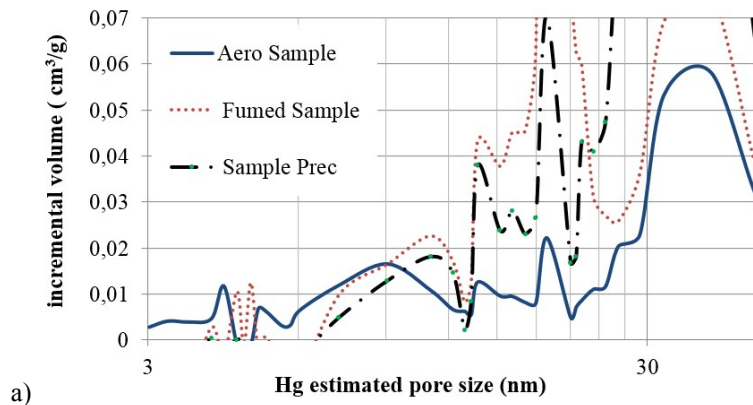
Supporting information

(SI)

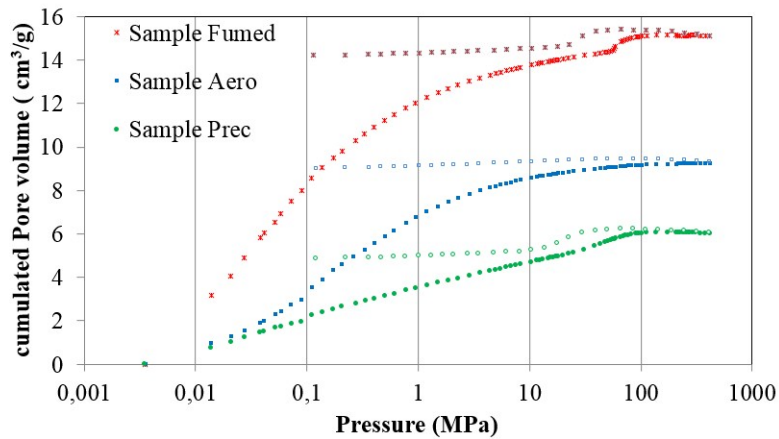
**Advanced three dimensional characterization of silica-based
ultraporous materials**



S1: BJH plot of pore size greater than 5nm determined by a BET analysis, Aero sample provide an accurate peak, other sample show a shoulder within the analyzed domain.



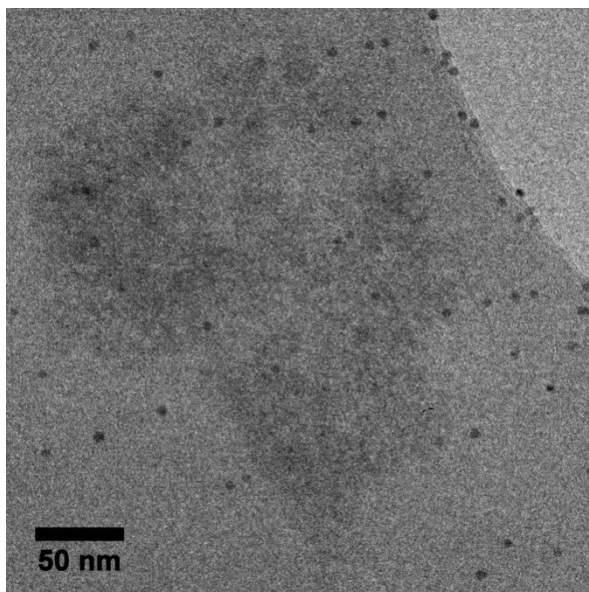
a)



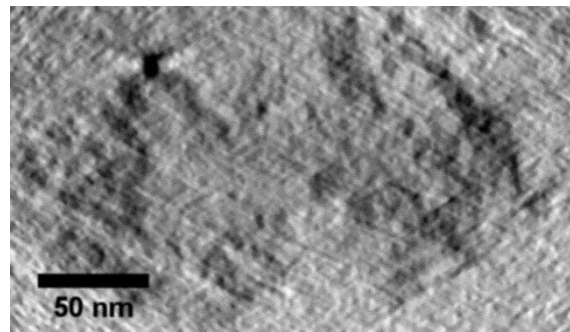
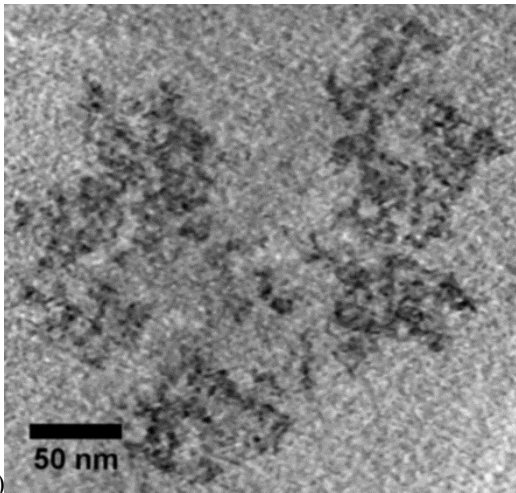
b)

S2: Mercury porosimetry on powder samples: (a) differential volume versus Hg estimated pore size (b) cumulated volume variation under mercury pressure loading up to 413 MPa followed by an unloading down to 0.1 MPa. Incremental volume confirmed that aero sample has smaller pore size than Prec. And Fumed below 10nm and equal pore size but less pore content for size greater than 10nm.

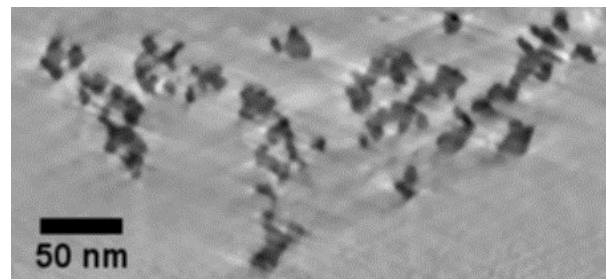
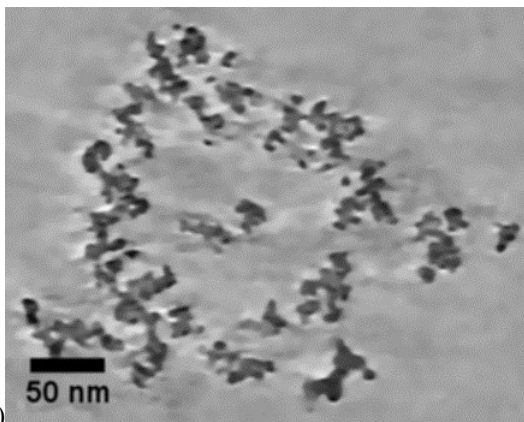
Advanced electron tomography (AET) tilt series were recorded in the low dose mode. The sample auto-tracking and auto-focusing were performed elsewhere than on the region of interest, preventing the beam damage.



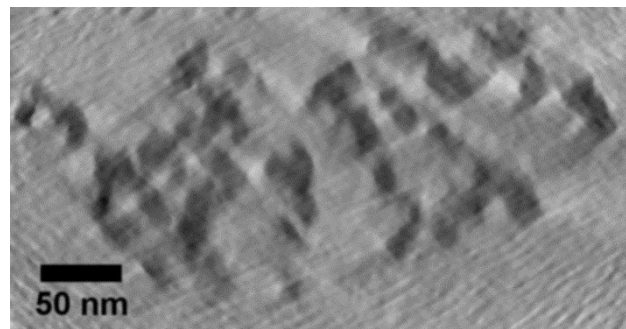
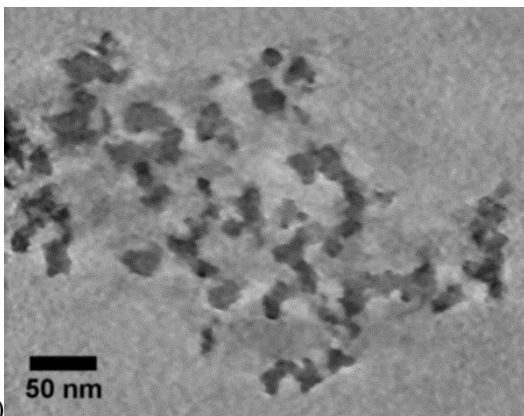
S3: Projection extracted from the tilt series recorded for Aero Sample at 0°. The minimum signal to noise ratio recorded in the projections is good enough to compute a volume with an exploitable gray level difference. The small black particles are the Au fiducial markers calibrated at 5 nm.



a)

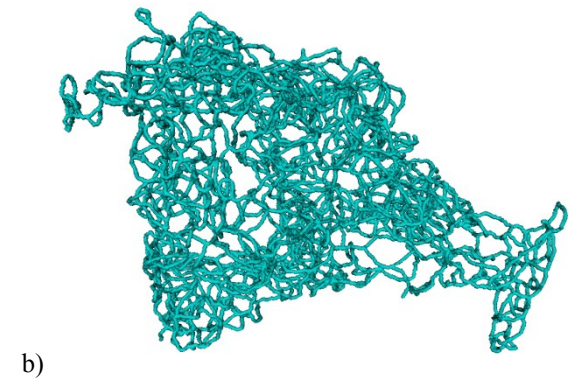
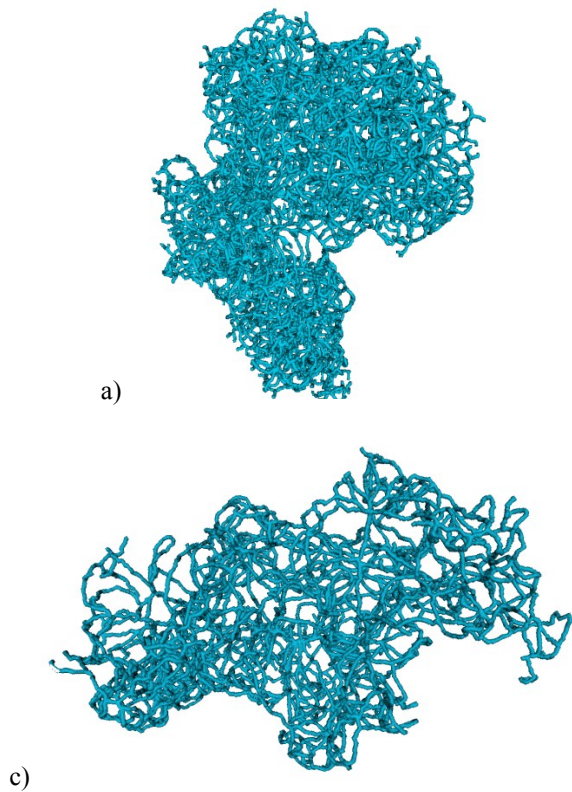


b)

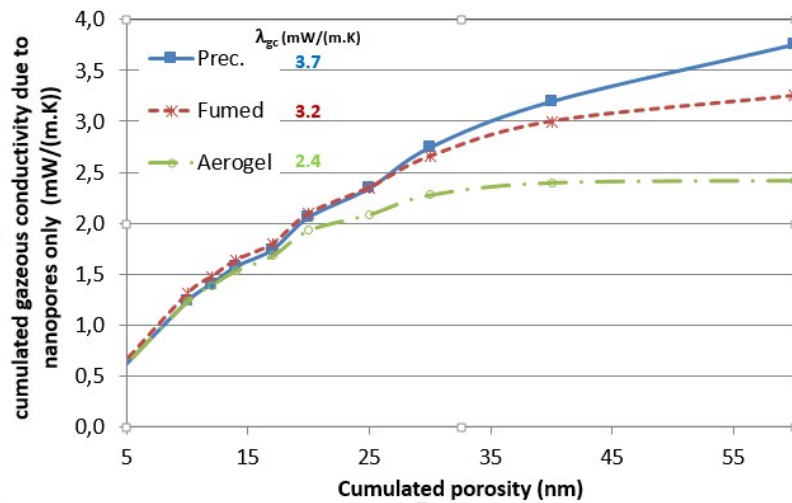


c)

S4 : Cross sections parallel to the XY (left) and XZ (right) plans extracted from the volume computed for the: a) Aero sample, b) Fumed sample and c) Prec sample. Dark gray dots represent silica particles and light grey dots characterizes the pore distribution. For all samples, the assembly of silica particles surrounding small pores can be observed. Bigger pores are then formed between aggregates.



S5: Porous network characterization for a) Aero Sample, b) Fumed sample and c) Prec. sample. The model of the porous skeleton were computed, showing that the porous network becomes less dense when the pore size increases, decreasing as well the number of connections between pores.



S6: Gas conductivity (λ_{cg}) calculation based on Knudsen law taking AET measurements as input for the pore size distribution. This confirmed that a decrease of the thermal conductivity by $3.7 - 2.4 = 1.3 \text{ mW}/(\text{m.K})$ can be obtained by working on synthesis parameters at the nanoscale.